



International Journal for Innovative Engineering and Management Research

A Peer Reviewed Open Access International Journal

www.ijiemr.org

COPY RIGHT



ELSEVIER
SSRN

2019 IJEMR. Personal use of this material is permitted. Permission from IJEMR must be obtained for all other uses, in any current or future media, including reprinting/republishing this material for advertising or promotional purposes, creating new collective works, for resale or redistribution to servers or lists, or reuse of any copyrighted component of this work in other works. No Reprint should be done to this paper, all copy right is authenticated to Paper Authors

IJEMR Transactions, online available on 16th Jan 2019. Link

[:http://www.ijiemr.org/downloads.php?vol=Volume-08/ISSUE-01](http://www.ijiemr.org/downloads.php?vol=Volume-08/ISSUE-01)

Title The influence of H₂ Gas in the formation of Porosity and Crack In Solution Precursor Plasma Spray Method

Volume 08, Issue 01, Pages: 354-363

Paper Authors

Mr. R. Sudarshan, Dr. K. Bala Subramanian, Dr.Sriram Venkatesh



USE THIS BARCODE TO ACCESS YOUR ONLINE PAPER

To Secure Your Paper As Per **UGC Guidelines** We Are Providing A Electronic Bar Code

The influence of H₂ Gas in the formation of Porosity and Crack In Solution Precursor Plasma Spray Method

Mr. R. Sudarshan¹, Dr. K. Bala Subramanian², Dr. Sriram Venkatesh³

¹ Geethanjali College of Engineering and Technology, Hyderabad

² Nonferrous Materials Technology Development Centre (NFTDC), Hyderabad

³ University College of Engineering, OU, Hyderabad

Corresponding: R. Sudarshan (rsujyo1@gmail.com)

Abstract: The porosity plays a significant role in the area of plasma spray coating for several engineering uses. Porosity is having its advantages and disadvantages in the coating functionality and also the instantaneous working atmosphere. The SS304 substrate was coated with the Zirconium based solution and observed the microstructures were with the help of SEM. The various parameters of spraying govern the porosity formation and development of plasma spray coating. Based on the changes in the parameters like current and H₂, the Zr coating's porosity, cracks, and thickness will vary. The size of the crack formation reducing with the increase of H₂ at the same current. The optimized spraying parameters are used to attain the foremost favourable coatings with minimal defects.

Key words: Porosity, Crack formation, SPPS, Microstructure, Zirconium based solution.

Introduction: The Solution Precursor Plasma Spray (SPPS) coating techniques have been widely utilized in surface engineering to ensure the systematic process and decrease the operation and maintaining price in several industries. Surface coatings are expanding in transporting companies like shipbuilding, marine structures, automobile and aeronautic discipline, production and tool-making industries, chemical and bio-medical industries, Etc. Coatings play an essential role in engineering by insulators against erosion, friction, and rust formation. They can be utilized for thermal shielding in high-temperature surroundings. Hence, which is required for preservation has given from every kind of corrosion, thus increasing dependability and higher efficiency of industrial elements. The porosity is one of the vital properties among the vital properties of plasma sprayed coatings, which can deteriorate the coatings' protection efficiency in hot operating conditions [3]. This research investigates

porosity development in SPPS coatings and the impacts of a variable group of coating parameters on porosity. Characterization and porosity estimation techniques of porosity in the coatings are epitomized depend upon the relevant research papers. In primary carrier gas, sometimes hydrogen is used to propel solution particles onto the prepared surface layer. In the aeronautics industry, thermal barrier coatings (TBCs) are widely used as heat shielding, oxidation resistance, clearance control coatings, evaporators, transition ducts, and stationary airfoils rotary airfoils, shrouded case for the abraded porous ceramics [4,5].

Surfaces, bond coat and ceramic top coat make up TBCs' standard three layers of construction. Before and after oxidation, as well as the thermally generated oxide layer that will form between top and bond coat, are shown in Figure 1.

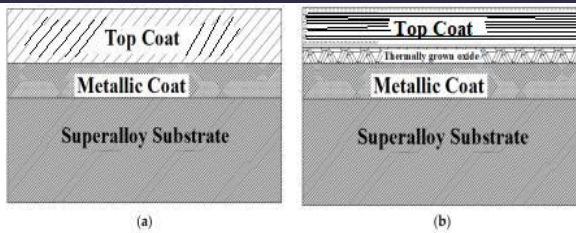


Figure 1. Showing the components of thermal barrier coating (TBC) (a) before oxidization (b) after oxidization with the inclusion of thermally grown oxide (TGO).

The development of continuous pores and microcracks in the topcoat of TBC allowed oxygen to pass through the bond coat at elevated temperatures in the course of operations and oxidized occurs [6]. Thermal Barrier Coating generally comprises a thermal insulating ceramic topcoat, a bond coat, and thermally generated oxide (TGO), which comes from the oxidation of metallic portions dispersed from the bond layer. [7]. During operation, the thermal mismatch stresses develop in such multi-layer composites [8], and initiation crack growth from defects in the TBC is likely. However, cracks that grow parallel to the spraying lamellae can cause spallation of TBC segments once they are long enough [9]. TBCs are splitting apart into layers or break off into fragments due to crack propagation and coalescence in the course of operation. This exposure causes the rotational components to fracture similarly to other components, which causes fatal problems. Few researchers have shown that the splitting apart into layers of TBCs occurs just above the interface between the topcoat and TGO layer [10,11–13]. Entrapped air sacks, voids and unmolten particles lead to different sizes and shapes of pores [14]. In the SPPS, particles impacting the substrate have various microstructures depending

upon the droplet trajectories in the gas flow [15]: Melted particles, hollow shells, and shell fragments. On the other hand, hollow and fractured shells generally come from not entirely polymerized droplets and travel on the plasma jet's fringes. Plasma spraying has many advantages, including creating fine microstructures that are non-columnar and have grains with similar axes. The ability to create relatively homogenous coatings that do not change in composition with thickness or deposition time, and the ability to process materials in virtually any surroundings. [16]. Plasma spraying can be used to create corrosion, erosion, temperature, and abrasion-resistant coatings and unchanging and near net forms while also taking advantage of the quick crystallization procedure. As long as the metal powder is glassy, it can be plasma-sprayed without altering its properties. For the deposition of high-temperature materials on substrates, plasma spraying has been employed for superconductive materials as a technique. Endoprostheses for orthopaedic trunks can now be coated with hydroxyapatite thanks to plasma spraying. [17]. As a result of plasma spraying, coatings are sprayed with many crevices, which allows the bone to grow into them. Some plasma coatings act as biocompatible layers, and in that titanium, bioactive hydroxyapatite coatings significantly promote normal layer formation into the layers of the delicate pores [18, 19]. Both fixed and flying gas turbines have been treated with sprayed coatings at different times and for different objectives [20]. Electrically conductive Al, Cu, and W and semi-conductive and insulating ceramic coatings are widely used in the electromechanical and computer sectors.

Some electrode contacts, such as the spark gaps of nuclear research equipment/tools, were made from enormous tungsten. Current electrodes can be replaced by tungsten electrodes sprayed with a 0.5mm thick tungsten coating. This electrode ensures that the short-span flows of 300,000Amp current with a life of many hundreds switching. [21, 22]. Water power plants, pump production, and pump operation are all areas where hydraulic devices could be used for a long time [23]. They are used in rolling mills and pressing industries to upgrade pricey heavy-duty equipment that would otherwise need to be replaced with expensive new designs. [24]. SS is used to rehabilitate 34 rolling strand journals by giving them an SS coating. NiCrBSi is used to renovate the blooming roll mill journal. 3/4 Gears of rolling mill gearbox being rebuilt with the help of wear resistance coating the manufacture of 3/4 Conveyor rollers in the plate has zirconia-based refractory coatings. 3/4 To repair a rolling mill slide and the plungers of a forging press, hard wear resistance is applied. Heat-resistant plasma coatings are commonly used in foundries and metallurgical equipment where molten metal or extremely high temperatures are encountered. The sliding plugs of steel ladles are integrated into this apparatus with alumina or zirconia coatings. Plasma spraying was also used on oxygen tubes and cast-iron moulds in continuous metals casting. [25]. Indirect contact with chemical reagents, the primary metals of machine elements are prone to a variety of wear and corrosion. In these situations, plasma coatings are utilized to protect the component's base metal. They will be used for different bearing surfaces, tubes,

furnaces, blades, shafts, sections of cooling equipment's, Etc. [26]. In the Czechoslovakian textile industry, plasma spraying was first employed. As an alternative to anodizing, chromium plating, and chemical surface hardening, plasma spraying has emerged as a viable solution. A wide range of critical equipment components can benefit from this technology. On equipment parts that come into contact with synthetic fibres, high-wear-resistant coatings are necessary. [27, 28]. Generally, the impacted parts of machinery are Filters, sieves, rolls, printing rolls and other printing machine parts. Because of its cost-effectiveness, the oxide layers are sprayed. Molten glass rapidly wears down the surface of the metal when it comes into contact with the metal. Plasma sprayed coatings are applied to metal instruments in order to maintain them. [30]. When possible, thermal spraying is suggested in the workshop for optimal results. Plasma spraying appears to be a versatile technique that has proven to be a reliable, cost-effective solution for various industrial difficulties in all thermal spray coating processes [31]. Unlike other thermal spraying methods, SPPS coatings have good characteristics based on their structural configurations. [32].

Experimental Setup:

In this paper, two different parameters, current and H₂ gas, have changed. At 300 amps and 400 amps current, the H₂ has changed in three levels (0, 20, & 40), and the spray distance is constant as 60mm. The parameters have given in table 1 has shown below.

Table1: Parameters

S.No.	Current (Amps)	Gas Flow		Spray Distance (mm)
		H ₂	Ar	
1	300	0	100	60
2		20	80	60
3		40	60	60
4	400	0	100	60
5		20	80	60
6		40	60	60

In this work, the above parameters are used for coating the solution precursor on SS304 substrate and observed the microstructures with different magnifications with the help of SEM and XRD is used to find out the existing elements and quantity of coating.

Results and Discussions:

The SPPS process is used for the solution precursor coating on the SS304 substrate at different parameters. The SEM and XRD results have been found and shown below.

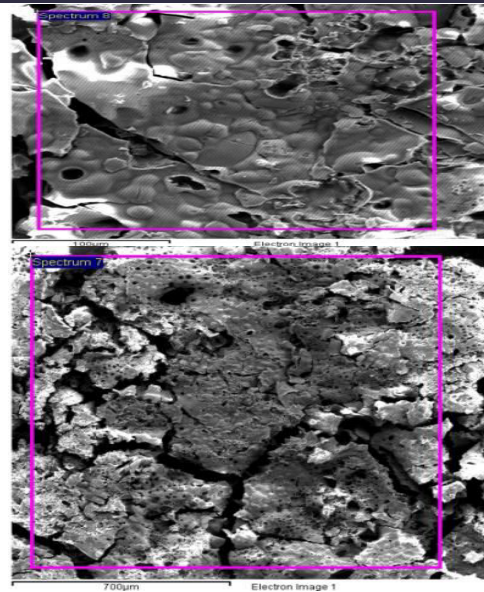


Figure 2. Microstructures of sample 1 at 300amps and 0 H₂

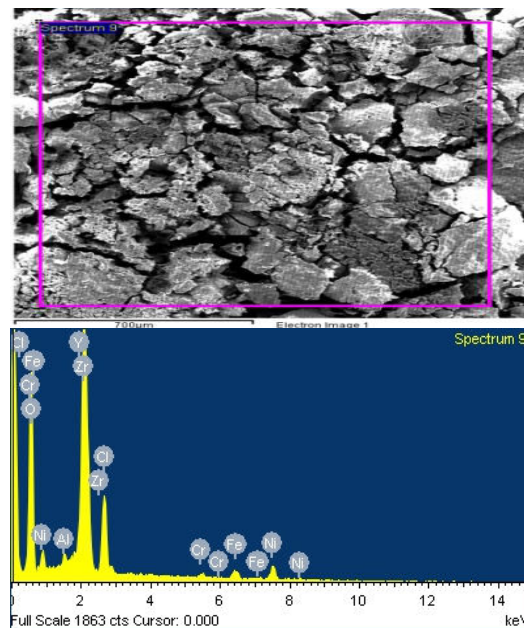


Figure.3. EDX and XRD of sample 1 at 300amps and 0 H₂

Element	Weight %	Atomic %
O K	52.42	82.54
Al K	0.55	0.51

Cl K	6.88	4.89
Cr K	0.60	0.29
Fe K	1.56	0.70
Ni K	3.60	1.55
Y L	2.90	0.82
Zr L	31.48	8.69
Totals	100.00	

From the observation of figures 2 & 3, microstructures showing that after spraying with argon without considering H₂, coarse pores are more as well as broad cracks are formed. By observing elemental table and XRD O to Zr deposition ratio is less. The coating thickness is also less.

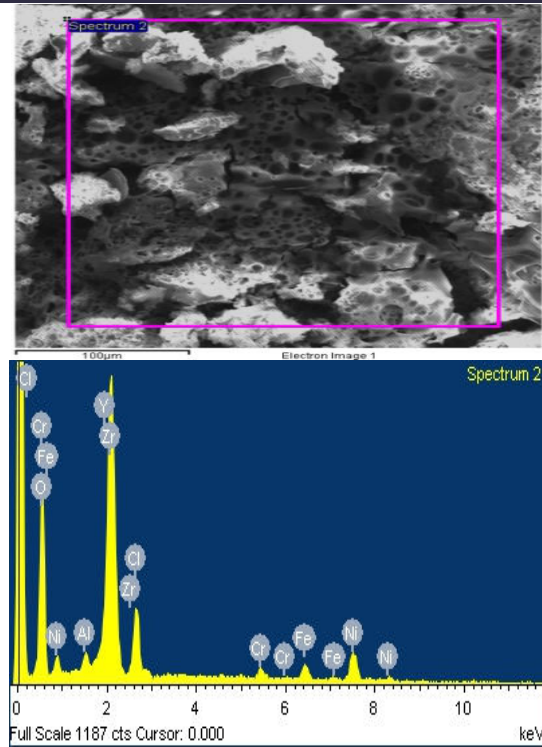


Figure 5. EDS and XRD of sample 2 at 300 amps and 20 H₂

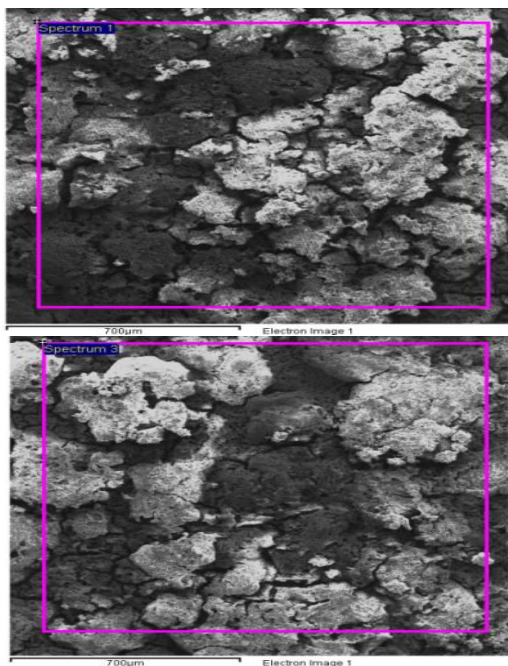


Figure.4. Microstructures of sample 2 at 300amps and 20 H₂

Element	Weight %	Atomic %
O K	46.73	79.06
Al K	0.77	0.77
Cl K	5.44	4.16
Cr K	1.27	0.66
Fe K	2.68	1.30
Ni K	7.50	3.46
Y L	3.83	1.17
Zr L	31.78	9.43
Totals	100.00	

After adding the 20 mpl of H₂ to argon , a clear change in the microstructure is

observed from figures 4 & 5. By observing microstructure fine porous formed with less crack width. By observing the elemental table the deposition ratio of O to Zr is increased. The thickness of coating is also increased.

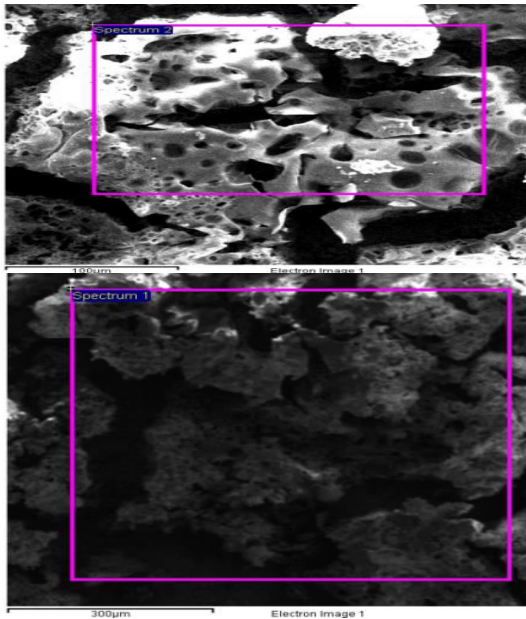


Figure 6. Microstructures of sample 3 at 300amps and 40 H₂

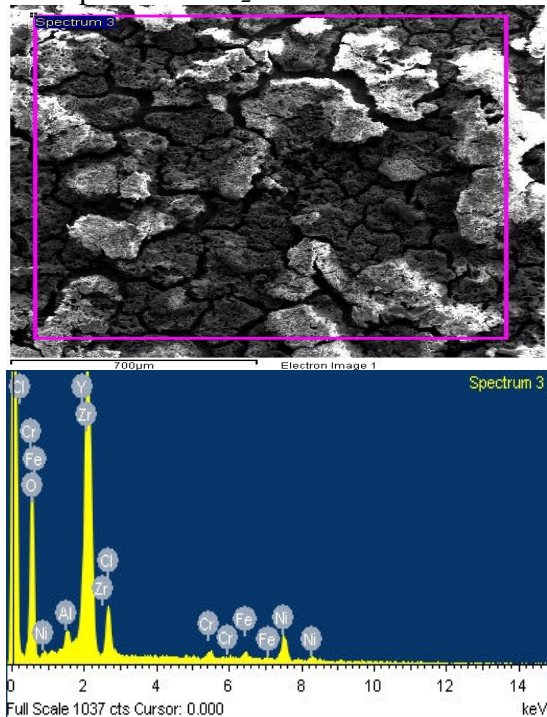


Figure.7. EDS and XRD of sample 3 at 300 amps and 40 H₂

Element	Weight %	Atomic %
O K	44.49	78.38
Al K	0.90	0.94
Cl K	4.43	3.52
Cr K	0.98	0.53
Fe K	1.29	0.65
Ni K	6.60	3.17
Y L	5.42	1.72
Zr L	35.90	11.09
Totals	100.00	

Increasing of H₂ to 40mpl it is observed that again the coarse pores are observed with mixed cracks i.e. some cracks width is more in some deposited areas where the Zr deposited very less even though the ratio of O to Zr is increased the constant thickness is not formed when we observing the microstructures. This leads to further investigation by increasing power to 400amp.

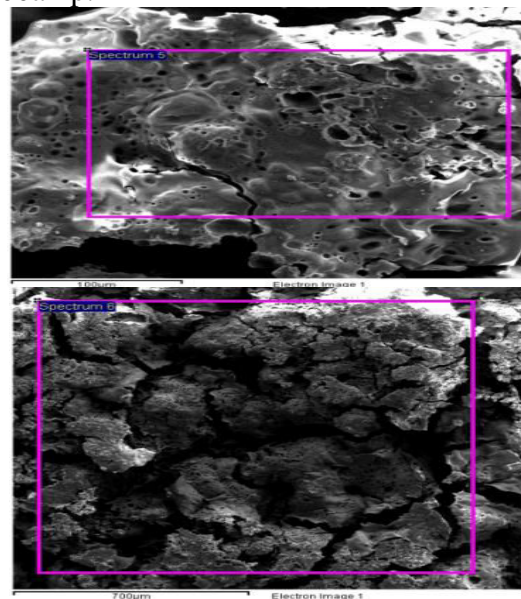


Figure 8. Microstructures of sample 4 at 400amps and 0 H₂

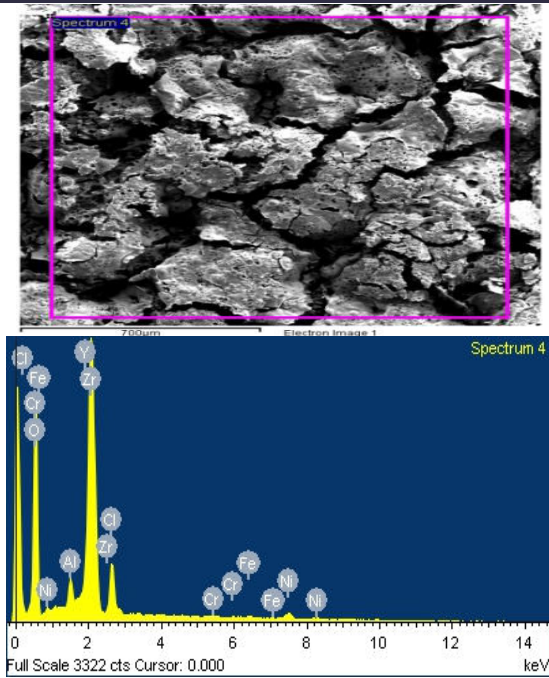


Figure.9. EDS and XRD of sample 4 at 400 amps and 0 H₂

Element	Weight %	Atomic %
O K	54.94	84.73
Al K	1.39	1.27
Cl K	4.42	3.08
Cr K	0.06	0.03
Fe K	0.24	0.11
Ni K	1.45	0.61
Y L	4.58	1.27
Zr L	32.91	8.90
Totals	100.00	

After increasing the power input deposition is more when compared with 300 amps input but the same coarse porous and wide cracks found.

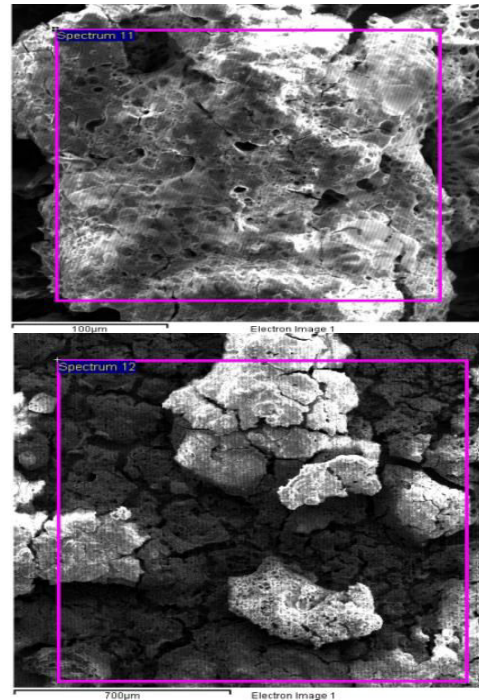


Figure .10. Microstructures of sample 5 at 400amps and 20 H₂

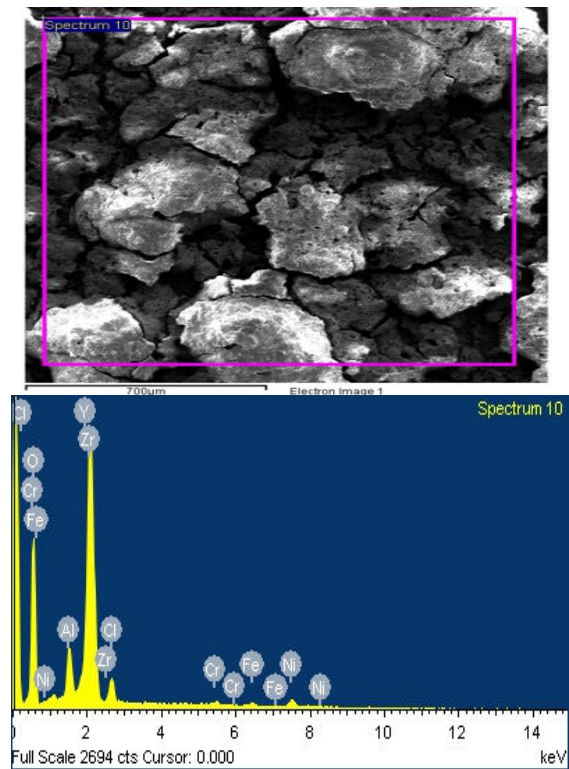


Figure.11 EDS and XRD of sample 5 at 400 amps 20 H₂

Element	Weight %	Atomic %
O K	50.82	82.36
Al K	3.03	2.91
Cl K	2.29	1.68
Cr K	0.46	0.23
Fe K	0.50	0.23
Ni K	2.31	1.02
Y L	5.59	1.63
Zr L	34.99	9.95
Totals	100.00	

After observing the microstructure, found the fine pores and fine cracks. The deposition ratio also increased simultaneously and the deposited thickness is even.

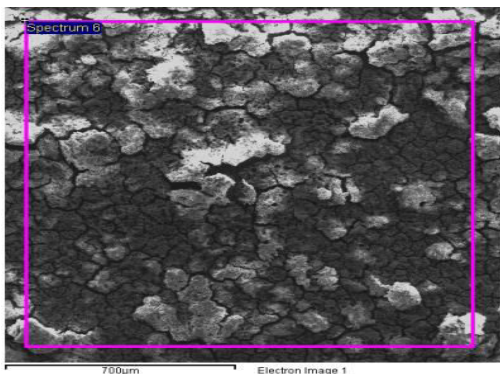
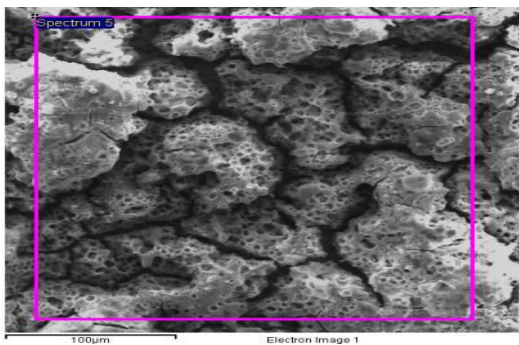


Figure.12. microstructure of sample 6 at 400 amps 40 H₂

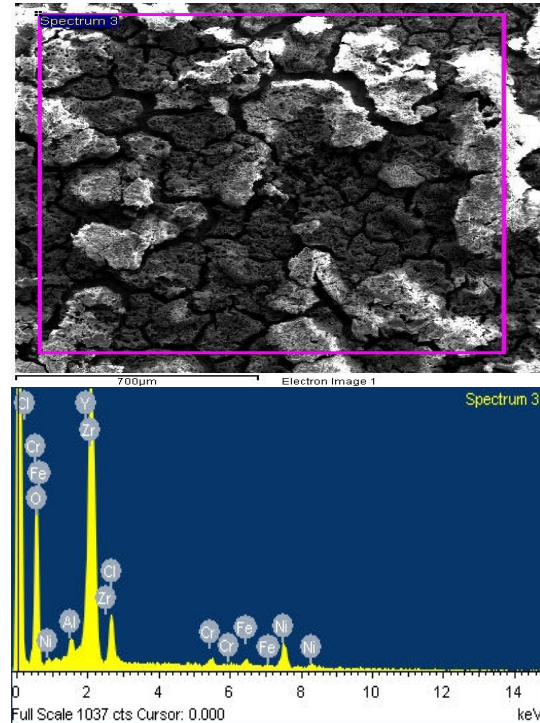


Figure.13. EDS and XRD of sample 6 at 400 amps 40 H₂

Element	Weight %	Atomic %
O K	45.61	79.38
Al K	1.96	2.02
Cl K	3.18	2.50
Cr K	0.85	0.45
Fe K	1.02	0.51
Ni K	3.74	1.77
Y L	6.39	2.00
Zr L	37.26	11.37
Totals	100.00	

After the power increase 40mpl H₂ is also given good result when compare with 300amps. The depotion ratio of O to Zr is increased. The coating thickness is also increased. Here the fine pores and fine cracks are found..

Conclusion:

In this paper, the research has taken place at two different current 300 and 400 amps but at the same different H₂ quantity 0, 20, 40 mpl. For the power 300 amps it is observed that 20 H₂ given good results when compare with 0 & 40 H₂. By means of deposited stabilization it is clearly showing that H₂ with Argon mix ratio will be near by 20 mpl. For 400 amps increasing os H₂ content also given fine pores and fine cracks. By observing all the microstructures it can be concluded that by increasing the power H₂ quantity also can be increased. By increasing the power and H₂ the thickness is also increased.

References:

1. Özel, S.; Vural, E. The microstructure and hardness properties of plasma-sprayed Cr₂O₃ J. Optoelectron. Adv. Mater. 2016, 18, 1052–1056.
2. Hermanek, F.J. Wear-Resistant Quasicrystalline Coating. U.S. Patent 6,254,699, 3 July 2001.
3. SchieflerFilho, M.F.O.; Buschinelli, A.J.A.; Gärtner, F.; Kirsten, A.; Voyer, J.; Kreye, H. Influence of process parameters on the quality of thermally sprayed X46Cr13 stainless steel coatings. J. Braz. Soc. Mech. Sci. Eng.2004, 26, 98–106.
4. Bennett, T.D.; Yu, F. A nondestructive technique for determining thermal properties of thermal barrier coatings. J. Appl. Phys. 2005, 97, 013520.
5. Chen, P.W.; Wang, S.M.; Wang, F.H. fracture analysis of thermal barrier coating delamination under thermalshock. Procedia Eng. 2015, 99, 344–348.
6. Daroonparvar, M.; Azizi Mat Yajid, M.; Yusof, N.M.; Sakhawat Hussain, M.

- Improved thermally grown oxide scale in air plasma-sprayed NiCrAlY/Nano-YSZ coatings. J. Nanomater. 2013, 2013, 520104.
7. Rabiei, A.; Evans, A. Failure mechanisms associated with the thermally grown oxide in plasma-sprayed thermal barrier coatings. Acta Mater. 2000, 48, 3963–3976.
8. T.W Clyne, S.C Gill, J. Thermal Spray Technol. 1996, 5. 401
9. S. R. Choi, J. W. Hutchinson, E.G. Evans, Mechanics of Materials, 31 (1999) 431
10. Rabiei, A.; Evans, A. Failure mechanisms associated with the thermally grown oxide in plasma-sprayed thermal barrier coatings. Acta Mater. 2000, 48, 3963–3976.
11. Zhou, Y.; Hashida, T. Thermal fatigue failure induced by delamination in thermal barrier coating. Int. J. Fatigue 2002, 24, 407–417.
12. Trunova, O.; Beck, T.; Herzog, R.; Steinbrech, R.; Singheiser, L. Damage mechanisms and lifetime behavior of plasma sprayed thermal barrier coating systems for gas turbines—Part I: Experiments. Surf. Coat. Technol.2008, 202, 5027–5032.
13. Khan, A.N.; Lu, J. Behavior of air plasma sprayed thermal barrier coatings, subject to intense thermal cycling.Surf. Coat. Technol. 2003, 166, 37–43.
14. R.Ghasemi, H. Vakilifard, Plasma-sprayed nanostructured YSZ thermal barrier coatings:Thermal insulation capability and adhesion strength, Ceramics International, 43 (2017) 8556-8563. 492
15. Saha A, Seal S, Cetegen B, Jordan E, Ozturk A and Basu S 2009 Thermo-physical processes in cerium nitrate precursor droplets injected into high temperature plasma *Surf. Coat. Technol.* **203** 2081–91.
16. National Materials Advisory Board, “Coatings for High-Temperature Structural Materials: Trends and Opportunities”, National Academy Press Washington D.C., <http://www.nap.edu/openbook/0309053811/html>, 1996.
17. A.W. Batchelor, L. N. Lam, M. Chandrasekaran,” Materials Degradation

and its Control by Surface Engineering”, 2nd Edition, Imperial College Press, London 2003.

18. <http://www.asbindustries.com/industry-applications/industries/medical-coatings>.

19. F. N. Longo, “Industrial guide- markets, materials, and applications for thermal-sprayed coatings”, *Journal Of Thermal Spray Technology*, Vol.1, No.2, 143-145, 1992, DOI: 10.1007/BF02659014.

20. P. Fauchais, J. F. Coudert, M. Vardelle, *J. De Physique IV*, 7, C 4–187, 1997.

21. <http://www.thermalsprayindia.com/Gas-Turbine.php>

22. B. V. Tilak, A. C. Ramamurthy and B. E. Conway, “High performance electrode materials for the hydrogen evolution reaction from alkaline media”, *Journal Of Chemical Sciences*, Vol. 97, N0. 3-4, 359-393, 1986, DOI: 10.1007/BF02849200.

23. Lynne M. Ernes, Richard C. Carlson, Kenneth L. Hardee, “Substrate of improved plasma sprayed surface morphology and its use as an electrode in an electrolytic cell”, Patent 5324407 Issued on June 28, 1994, Filing date: Feb 26, 1993.

24. <http://www.edisonsa.co.za/thermalspraying.htm>

33.

25. <http://www.ec21.com/product-details/Aluminium-Foil-Roll--6584377.html>

26. Pierre D'Ans, Jean Dille, Marc Degrez, “Thermal fatigue resistance of plasma sprayed yttria-stabilised zirconia onto borided hot work tool steel, bonded with a NiCrAlY coating:81Experiments and modeling”, *Surface and Coatings Technology*, Vol. 205, Issue 11, 3378- 3386, 2011.

27. Robert B. Heimann, “Plasma-Spray Coating: Principles and Applications”, 1996, ISBN 3- 527-29430-9

28. RamnarayanChattopadhyay, “Advanced Thermally Assisted Surface Engineering Processes”, 2004, ISBN 1-4020-7696-7.

29. <http://www.textiletoday.com.bd/magazine/printable.php?id=175>

30. <http://www.indiamart.com/plasmaapplication-processor-s/thermal-spraying.html>

31. http://nxedge.supremeserver23.com/is_glass_industry.php

32. E. Brinley, K. S. Babu, S. Seal, “ The Solution Precursor Plasma Spray Processing of Nanomaterials “ 54 - 59, *J.O.M*, July, 2007.